Title

Punctiform and Polychromatic Pre-Descemet Corneal Dystrophy: Clinical Evaluation and Identification of the Genetic Basis

Authors

Alió Del Barrio, Jorge L
Chung, Doug D
Al-Shymali, Olena
et al.

Publication Date

2020-04-01

DOI

10.1016/j.ajo.2019.11.024

Peer reviewed

HHS Public Access

Author manuscript

Am J Ophthalmol. Author manuscript; available in PMC 2021 April 01.

Published in final edited form as:

Am J Ophthalmol. 2020 April ; 212: 88–97. doi:10.1016/j.ajo.2019.11.024.

Punctiform and Polychromatic Pre-Descemet Corneal Dystrophy: Clinical Evaluation and Identification of the Genetic Basis

Jorge L. Alió del Barrio, MD, PhD[1,2], **Doug D. Chung, PhD**[3], **Olena Al-Shymali, MD**[1], **Alice Barrington**[3], **Kavya Jatavallabhula**[3], **Vinay S. Swamy**[3], **Pilar Yébana, OD**[1], **Maria Angélica Henríquez-Recine, MD**[4], **Ana Boto-de-los-Bueis, MD, PhD**[4], **Jorge L. Alió, MD, PhD**[1,2], **Anthony J. Aldave, MD**[3]

[1]Cornea, Cataract and Refractive Surgery Unit, Vissum Corporación, Alicante, Spain.

[2]Division of Ophthalmology, School of Medicine, Universidad Miguel Hernández, Alicante, Spain.

[3]Stein Eye Institute, David Geffen School of Medicine at UCLA, Los Angeles, California, USA.

[4]Ophthalmology Department, La Paz University Hospital, Madrid, Spain.

Abstract

Purpose—To report the clinical features and genetic basis of three previously unreported families with punctiform and polychromatic pre-Descemet corneal dystrophy (PPPCD).

Design—Observational case series.

Methods—Full ophthalmic assessment was performed for members of three unreported families with PPPCD. Structural and biomechanical alterations of the cornea were screened. Whole-exome-sequencing (WES) was performed on the first family. Novel or rare variants that segregated with the affected status were screened for in the other two families with Sanger sequencing. Identified variants that segregated with the affected status in all families were characterized using in silico prediction tools and/or in vitro splice assays. Additionally, two previously reported PPPCD families were screened for variants identified in the three unreported PPPCD families.

Results—Twelve of 21 examined members of the three unreported families were diagnosed with PPPCD. The only refractive, topographic or biomechanical abnormality associated with PPPCD was a significantly increased corneal stiffness. WES and Sanger sequencing identified two variants that segregated with the affected status in the all three families: a rare intronic *PDZD8* c.872+10A>T variant and a novel missense *PRDX3* c.568G>C (p.Asp190His) variant. The same

Corresponding Author: Anthony J. Aldave, MD., Professor of Ophthalmology. Stein Eye Institute. 200 Stein Plaza, UCLA. Los Angeles, CA 90095-7003. Tel: 310.206.7202. Fax: 310.794.7906. aldave@jsei.ucla.edu.

Conflict of interest: No financial disclosures. The authors, their families, their employers and their business associates have no financial or proprietary interest in any product or company associated with any device, instrument or drug mentioned in this article. The authors have not received any payment as consultants, reviewers or evaluators of any of the devices, instruments or drugs mentioned in this article.

PRDX3 variant was identified in the previously reported PPPCD family expressing the common PPPCD phenotype, and is predicted by in silico prediction tools to be damaging to protein function.

Conclusions—PPPCD is associated with an alteration of corneal biomechanics and a novel missense variant in *PRDX3.* Screening of additional families will determine whether all families demonstrate a *PRDX3* variant, or whether locus heterogeneity may exist for PPPCD.

Keywords

Corneal dystrophy; punctiform; polychromatic; genetics; cornea

INTRODUCTION

Punctiform and polychromatic pre-Descemet corneal dystrophy (PPPCD) is a rare corneal dystrophy first described by Fernandez-Sasso et al in 1979.[1] Typically asymptomatic without any reported visual disturbance, PPPCD is characterized by the presence of punctiform, multicolored opacities in the posterior stroma, immediately anterior to Descemet membrane.[1–7] According to the second edition of the IC3D classification of corneal dystrophies, PPPCD is currently considered a subtype of pre-Descemet corneal dystrophy (PDCD), which is classified as a "Category 4" dystrophy (suspected, new, or previously documented corneal dystrophies, where the evidence for it being a distinct entity is not yet convincing).[8]

To our knowledge, only ten families with PPPCD have been reported in the literature as case reports (Table 1).[1–7] While an autosomal dominant inheritance has been suggested, the inheritance pattern and genetic basis have yet to be elucidated. Additionally, it is also unknown whether PPPCD is associated with any other corneal abnormalities as a complete ophthalmic assessment of individuals with PPPCD has not been reported.

We present three previously unreported PPPCD pedigrees, in which we performed a comprehensive ophthalmic assessment of affected and unaffected family members, as well as the results of whole exome and Sanger sequencing in these and two previously reported pedigrees to identify the genetic basis of PPPCD.

MATERIALS AND METHODS

Three previously unreported (PPPCD family 1, family 2 and family 3) and two previously reported (PPPCD family 4 and family 5)[7] PPPCD pedigrees were identified and family members enrolled in this observational case series and in the authors' ongoing study of inherited ocular disorders. Informed written consent was obtained from all subjects in this study according to the tenets of the Declaration of Helsinki and approval for this study was obtained from the Institutional Review Board at the University of California at Los Angeles (UCLA IRB#11–000020) and the ethical committee from Vissum Corporación.

Clinical Evaluation

All affected and unaffected individuals from three previously unreported families (PPPCD family 1–3) that agreed to participate in the study received a full ophthalmic examination including: slit lamp biomicroscopy, fundoscopy, corneal endothelial specular microscopy (Noncom Robo, Japan), corneal topography (including anterior keratometry, pachymetry and corneal aberrometry with 6-mm pupil) (Sirius, CSO, Italy), ocular aberrometry (Osiris, CSO, Italy), anterior segment optical coherence tomography (AS-OCT) (MS-39, CSO, Italy), corneal biomechanics (Ocular Response Analyser, OftalTech, Spain) and ocular scattering index (OSI) (HD Analyzer, Visiometrics, Spain). Affected individuals also underwent corneal confocal biomicroscopy (Confoscan 4, Nidek, Japan). Two individuals under 5 years of age were included in the study, but due to the expected lack of cooperation, only a clinical examination (slit lamp examination and fundoscopy) was performed. The diagnosis of PPPCD was based on the presence of polychromatic crystals located into the posterior corneal stroma (in a pre-Descemet membrane location) on slit lamp examination that appeared as hyperreflective pre-Descemetic opacities with confocal and specular microscopy (Figures 1 and 2).

Although a comprehensive past medical history, including a complete medication history, was taken from each of the individuals recruited into the study, a physical examination to identify systemic or metabolic associations was not performed given the last of evidence of extraocular manifestations of PPPCD in previous reports.[1–7]

Statistical Analysis

SPSS software for Windows was used for statistical analysis (IBM SPSS Statistics, version 22.0). Analysis was performed for all variables with non-parametric tests due to the small sample size ($n<30$). Thus, the Mann-Whitney test was applied to assess differences between groups (affected and unaffected), except for the nominal variable “sex”, for which the Pearson’s chi-squared test (X^2 test) was used. Differences were considered statistically significant when $p<0.05$.

DNA isolation

After informed consent was obtained, saliva samples were collected from members of each of the three unreported families and the two previously reported families[7] with the Oragene Saliva Collection Kit (DNA Genotek, Inc., Ottawa, Canada) and genomic DNA was isolated using the Oragene prepIT-L2P Kit (DNA Genotek, Inc.) according to the manufacturer’s instructions.

WES and variant calling

WES was performed on genomic DNA derived from affected and unaffected members of PPPCD family 1. DNA libraries were prepared using the TruSeq DNA Sample Preparation Kit v2 (Illumina Inc., San Diego, CA) and exome capture was performed with the SeqCap EZ Exome Library v3.0 (Roche NimbleGen, Inc., Madison, WI). Paired-end sequencing (2×150 bp) was performed with Illumina’s HiSeq 4000 by Genewiz (South Plainfield, NJ). Using the Qiagen’s Biomedical Genomics Workbench 5.0 (Qiagen, Redwood City, CA), the generated sequence reads were aligned to the Hg38 human genome reference, and aligned

reads were annotated with the Ensembl 88 transcript database. Called variants were annotated with the dbSNP 150 database.

Filtering of WES variants

Using Qiagen's Ingenuity Variant analysis software, variants identified by WES analysis in the affected and unaffected members of PPPCD family 1 were filtered to exclude any variant with: a quality score < 20, read count < 5, or minor allele frequency (MAF) > 0.5% in either the ExAC, 1000genomes, or genomeAD databases; present in a homozygous state; absent in any of the affected individuals; and present in any of the unaffected individuals. To make allowances for a potential false positive/negative call by WES for any particular variant in one individual, additional filtering and analyses were performed to exclude variants: absent in 2 or more of 6 affected and present in any unaffected individuals; or absent in any of the affected individuals and present in 2 or more of 4 unaffected individuals.

PCR amplification and Sanger sequencing

Primers were designed to amplify the genomic regions containing: filtered variants identified by WES; exons and/or introns of *PDZD8* (Refseq Gene ID: 118987), *PRDX3* (Refseq Gene ID: 10935), and *OR2M5* (Refseq gene ID: 80000) (see Supplemental Table 1 for primer sequences); and variants used for mini-haplotype analysis. DNA amplification by polymerase chain reaction (PCR) was performed in 25μL reaction volumes containing 25–40 ng of genomic DNA, 2.5 pico-moles of each primer, and GoTaq® Green Master mix (Promega, Madison, WI) according to the manufacturer's recommendations. The PCR protocol consisted of a denaturizing step at 95°C for 3 minutes, followed by a 35x cycle of: a denaturing step at 95°C for 30 seconds, annealing step at 60°C for 30 seconds, and elongation step at 72°C for 30–60 seconds. Sanger sequencing was performed by Laragen, Inc. (Culver City, CA).

In silico variant prediction and scoring

Filtered variants identified by WES were analysed by online tools SIFT[9], Polyphen-2[10], CADD[11, 12], Provean[13], and/or Human Splicing Finder[14] to predict each variant's impact on protein function or splicing.

Mini-haplotype analyses

To determine the haplotype of the genomic region encompassing the *PRDX3* c.568G>C variant on chromosome 10, rare proximal variants were identified in the WES data from PPPCD family 1 and screened in affected individuals from families 2–4 who harboured the *PRDX3* c.568G>C variant (see Supplemental Table 1 for primer sequences).

In vitro splice assay

A 1444 bp region of *PDZD8,* containing either the wild-type sequence or the c.872+10A>T variant, was amplified from genomic DNA obtained from either an affected or unaffected individual of PPPCD family 1. The amplified *PDZD8* fragment contained exon 1, along with 264 bp of the 5' UTR and 308 bp of intron 1 that flank exon 1, and was amplified using the following primer sequences: Forward- 5'-GAATT

CCCATATGGAGTGGAGGCCTGAGGGA-3' and Reverse- 5'-GAATTCCCATATGCCTGGGGATTAGGGTAGGCT-3'. Both primers were designed with a Ndel restriction site at their 5' ends to be used for cloning the amplified *PDZD8* fragment into the pTBNde(min) plasmid (plasmid# 15125, a gift from Franco Pagani, Addgene, Cambridge, MA) that contains a modified version of the α-globin-fibronectin-EDB minigene.[15, 16]

The splicing assay was performed by transfecting HEK293T cells with each minigene plasmid using Lipofectamine® LTX (Life Technologies, Grand Island, NY) according to the manufacturer's recommended protocols. Total RNA from transfected HEK293T was extracted using TRI Reagent (Sigma-Aldrich Corp., St. Louis, MO) and complementary DNA (cDNA) was synthesized using the Superscript Ill First-Strand kit (Life Technologies) according to the manufacturer's recommendations. Reverse transcription PCR (RT-PCR) was performed using previously published RT-PCR protocols with primers targeting the flanking fibronectin exons (see Supplemental Table 1 for primer sequences).[17]

RESULTS

Clinical evaluation of PPPCD families

Seventeen members from family 1, six members from family 2 and two members from family 3 were enrolled in the clinical study (Figure 1). Slit lamp examination demonstrated bilateral, symmetric, punctiform and polychromatic opacities in the deep stroma immediately anterior to Descemet membrane in eight individuals from family 1, three individuals from family 2, and one individual from family 3 (Figures 1 and 2). There was no significant difference in the mean age between the affected (42.9 years; range 8–79) and unaffected (33.3 years; range 1–69) individuals (p= 0.25) or in the percentage of men in the affected (41.6%; 5/12) and unaffected groups (53.8%; 7/13; p= 0.38).

Comprehensive clinical examination failed to reveal associated ophthalmic disorders in the affected individuals. In addition, no ophthalmic surgical interventions were documented in any of the study patients' medical records, with an exception of bilateral cataract surgery in an affected 79-year-old individual. Corneal imaging could not be performed due to limited cooperation in two patients: a 4-year-old child (unaffected based on slit lamp examination) and a 1-year-old infant (unaffected based on a portable slit lamp examination).

Anterior Segment Imaging

Anterior segment OCT imaging of the corneas of affected individuals demonstrated faint, hyperreflective, pre-Descemetic opacities (Figure 3-top), which were more easily visualized with Scheimpflug imaging (Figure 3-bottom). These opacities were absent in the unaffected individuals.

Specular and confocal microscopic imaging

Specular microscopic imaging of the corneal endothelium revealed a normal endothelial cell mosaic in both groups, with similar cellular density, coefficient of variation and percentage of hexagonality (Table 2). Affected individuals demonstrated multiple, round,

hyperreflective opacities at the pre-Descemetic level, immediately anterior to an unremarkable endothelial cell layer (Figure 4-right). Confocal microscopic imaging of affected individuals demonstrated an unremarkable corneal stroma other than for the extracellular, pre-Descemetic opacities that measured approximately 10μm in diameter (Figure 4-left).

Cornea biomechanics

Corneal biomechanical evaluation demonstrated increased corneal hysteresis (CH; p=0.26) and significantly increased corneal resistance factor (CRF; p=0.02) in individuals with PPPCD compared with unaffected individuals (Table 2).

Vision, refraction and corneal topography

There were no statistically significant differences in any of the other analysed visual, refractive, keratometric, pachymetric or corneal aberrometric parameters (Table 2).

WES analysis of PPPCD family 1

DNA samples were collected from 13 members (8 affected and 5 unaffected) of PPPCD family 1 (Figure 1A). WES was performed on DNA samples from six affected (II:6, III:7, III:11, III:13, IV:4, IV:8) and four unaffected individuals (III:5, III:8, III:9, III:14). After excluding variants with low quality (quality score < 20) and low read counts (read counts < 5), 281,004 unique variants (SNV and indels) were collectively identified in the 10 individuals. After excluding homozygous variants (given the observed autosomal dominant inheritance pattern in PPPCD family 1), 108,844 heterozygous variants were evaluated for allele frequency, revealing that 29,336 were novel or rare (MAF < 0.5%). After filtering variants based on segregation with the affected phenotype, no novel or rare heterozygous coding region variants were present in all 6 affected individuals and not present in any of the 4 unaffected individuals. While WES primarily targets the coding regions of the genome, the non-coding regions of the genome that are close to intron-exon junctions are also typically captured and sequenced. As such, screening of the 29,336 novel or rare heterozygous variants revealed two intronic variants, *PDZD8* c.872+10A>T (based on transcript NM_173791.4) and *GREB1L* c.4229–25T>C (based on transcript NM_001142966.2), that segregated with the affected phenotype in the 10 members of PPPCD family 1 who underwent WES (Table 3). Sanger sequencing performed to validate the WES results for these two intronic variants confirmed the results of WES in each of the 10 individuals. Sanger sequencing of *PDZD8* and *GREB1L* in the remaining three individuals of PPPCD family 1 who did not undergo WES (III:15, IV:6, IV:9) demonstrated that *PDZD8* c.872+10A>T continued to segregate with the affected status while *GREB1L* c.4229–25T>C did not.

To allow for a false positive/negative call by WES for any particular variant in one individual, re-analysis of the WES data was performed using less stringent criteria for filtering variants (see Methods), which led to the identification of: 8 heterozygous novel or rare coding region variants present in 5 of 6 affected individuals and not present in any of the 4 unaffected individuals; and 3 heterozygous rare coding region variants present in 6 of 6 affected individuals and not present in more than 1 unaffected individual (Table 3). Sanger

sequencing validation of these 11 total coding region variants did not identify any false positives; however, Sanger sequencing revealed 3 variants, *OR2M5* c.773T>C, *PRDX3* c.568G>C and *LAMA3* c.1571G>A, to be false negatives in one of the 6 affected individuals, thereby confirming each of these three variants to be present in all 6 affected individuals and not present in any of the 4 unaffected individuals. Sanger sequencing screening in the three additional family members who did not undergo WES revealed *OR2M5* c.773T>C and *PRDX3* c.568G>C continued to segregate with the affected status while *LAMA3* c.1571G>A did not (Table 3). The *OR2M5* c.773T>C variant was predicted by SIFT to have an activating impact on protein function but was predicted to be benign or neutral by PolyPhen and Provean (Table 3). In contrast, *PRDX3* c.568G>C variant was predicted by SIFT, PolyPhen and Provean to deleteriously impact protein function, and also obtained a CADD score of 31, which places this variant in the top 0.1% of deleterious substitutions in the human genome (Table 3).[12]

Screening of PDZD8, PRDX3, and OR2M5 in PPPCD families 2 and 3

Given that *PDZD8* c.872+10A>T, *OR2M5* c.773T>C, and *PRDX3* c.568.G>C segregated with the affected status in PPPCD family 1, we performed Sanger sequencing of all three genes in three affected (I:1, II:1, II:4) and two unaffected (I:2, II:2) members of PPPCD family 2 and in one affected individual (II:1) and one unaffected individual (II:3) in PPPCD family 3 (Figure 1B and 1C). Sanger sequencing of the *OR2M5* coding region did not reveal a novel or rare variant in either family 2 or family 3. Sanger sequencing of *PDZD8* and *PRDX3* revealed the same *PDZD8* c.872+10A>T and *PRDX3* c.568G>C variants identified in PPPCD family 1 in the heterozygous state in the affected individuals and absent in the unaffected individuals of family 2 and family 3. The *PDZD8* and *PRDX3* variants are both located on chromosome 10 within ~2Mb from each other. Based on a previously performed RNA- seq analyses of adult human corneal gene expression, both *PDZD8* and *PRDX3* are expressed in ex vivo keratocytes and endothelial cells, with RPKM values of: 4.25 and 8.67 for *PDZD8,* respectively; and 8.43 and 33.91 for *PRDX3,* respectively.[18]

Impact of PDZD8 c.872+10A>T on splicing

In silico analysis performed using Human Splicing Finder v3.1 predicted that the *PDZD8* c.872+10A>T variant activates an intronic cryptic donor splice site, potentially altering splicing. To determine whether the *PDZD8* c.872+10A>T variant does in fact alter splicing, an in vitro splice assay was performed by inserting a genomic sequence containing the *PDZD8* exon 1 and partial intron 1 (either with the c.872+10A>T variant or the wild-type sequence) in between two flanking fibronectin 1 *(FN1)* exons residing within a *FN1* minigene plasmid, which was subsequently transfected into HEK293T cells. Using cDNA generated from the transfected HEK293T cells, RT-PCR demonstrated the c.872+10A>T variant caused the loss of a transcript-splice product (denoted by a ~700bp band) that was detected in the *FN1/PDZD8* minigene with the wild-type sequence (Supplemental Figure 1). Sequencing of the ~700bp band revealed the c.325 to c.872 region of *PDZD8* exon 1 spliced in between the two flanking *FN1* exons. Sequencing of the ~1400bp and ~400bp bands revealed transcript products, flanked by the two minigene *FN1* exons, containing either: the *PDZD8* 5'UTR and exon 1 regions; or a *FN1* exonic region (c.3797–4064, NM_212482), respectively (Supplemental Figure 1).

Screening of PRDX3, PDZD8, and OR2M5 in two previously published PPPCD families

Genomic DNA samples were obtained from members of two previously reported PPPCD families: 3 affected individuals from PPPCD family 4 and 7 affected individuals from PPPCD family 5.[7] Screening of the *PDZD8* exon1/intron1 region in each of the affected individuals from both families did not reveal the c.872+10A>T variant. Screening of the *PDZD8* promoter and coding regions and the *OR2M5* coding region in two affected individuals from both families failed to reveal a novel or rare variant. Screening of the *PRDX3* coding region in each of the affected individuals from both families identified the same c.568G>C variant in all three of the affected individuals of PPPCD family 4 but did not identify a novel or rare variant in PPPCD family 5.

Identification of ancestral mini-haplotype in families 1–3

Rare variants that are adjacent to the *PRDX3* c.568G>C variant were genotyped in the four PPPCD families that demonstrated the *PRDX3* c.568G>C variant to determine whether this variant likely arose from a common ancestor (Supplemental Figure 2). The same mini-haplotype was identified in the three previously unreported families (PPPCD families 1, 2, and 3) but not in PPPCD family 4, suggesting that the *PRDX3* c.568G>C variant likely arose from a common ancestor in PPPCD families 1–3 and independently in PPPCD family 4.

DISCUSSION

The aim of this study was to perform a through corneal phenotypic analysis and to elucidate the genetic basis of punctiform and polychromatic pre-Descemet corneal dystrophy after the identification of three unreported families. In order to corroborate the results of genetic analysis in these three families, we recruited members of two recently reported families for additional screening.[7] One of these families (Family 4) demonstrated the typical PPPCD phenotype, with localization of the opacities to the pre-Descemetic posterior stroma, as was observed in the three unreported families. However, affected members of family 5 presented an atypical PPPCD phenotype in that the opacities were distributed throughout all levels of the corneal stroma, indicating that this family may have a dystrophy that is clinically and genetically distinct from *PRDX3*-associated PPPCD.[7] What is common to each of these five families, and indeed to eight of the 13 families reported to date is location in Spain or Spanish ancestry (Table 1). In addition, four of the five other families reported to date have been in Brazil (family origin non reported). Considering that Brazil and all South America have received strong immigration from the Iberian peninsula since the XVI century after the discovery of America, it is likely that the causative mutation(s) originated in the Iberian peninsula centuries ago.

Our investigation identified two variants, *PRDX3* c.568G>C and *PDZD8* c.872+10A>T, that segregated with the affected status in multiple PPPCD pedigrees. *PRDX3* c.568G>C (p.Asp190His) is novel (not reported in the dbSNP database) and was identified in 4 of 5 pedigrees affected with PPPCD, with haplotype analysis indicating that this variant likely derived from an independent event in family 4. However, given the ~2 Mb distance between the two variants, we cannot rule out the possibility the *PRDX3* c.568G>C variant arose from the same founder in all four families. The *PDZD8* c.872+10A>T variant, identified in 3 of 5

PPPCD families, is not novel but is rare, and was demonstrated to impact splicing in vitro; whether or not splicing is altered in vivo by this variant, and is not simply an artifact of the in vitro splice assay, is yet to be determined. However, each of these 3 families in which it was identified also demonstrated the *PRDX3* c.568G>C variant, which is only ~2Mb away from *PDZD8* c.872+10A>T variant. Therefore, it is likely that these two variants on chromosome 10, along with the other rare variants within the shared mini-haplotype, were inherited from a common ancestor in PPPCD families 1–3. Given that both *PRDX3* c.568G>C and *PDZD8* c.872+10A>T were identified in PPCD families 1–3 that likely share a common ancestor but the novel *PRDX3* c.568G>C variant was also found in a fourth unrelated PPPCD pedigree, *PRDX3* is likely the causative gene for PPPCD.

The *PRDX3* gene belongs to the thioredoxin family of peroxidases and encodes a mitochondrial antioxidant peroxidase that is responsible for regulating mitochondrial reactive oxygen species (mROS).[19–21] Overexpression of *PRDX3* has been reported in various cancers, while knockdown of *PRDX3* was demonstrated to increase mtDNA oxidation and silencing of *PRDX3* promoted enhanced invasive properties in HepG2 cells.[22–26] Interestingly, a significant decrease of PRDX3 protein expression was reported in corneal endothelium derived from patients affected with Fuchs endothelial corneal dystrophy (FECD) compared to healthy controls, suggesting that corneal endothelial cells affected with FECD are less able to withstand oxidant-induced damage, possibly contributing to the pathogenesis of the disease.[27] In the same report, while PRDX3 protein was shown to be expressed in normal corneal endothelium, PRDX3 protein was demonstrated to not be expressed in either normal corneal stroma or epithelium.[27] While our identification of *PRDX3* expression in ex vivo human corneal endothelial cells using RNA-seq corroborates this report, we found *PRDX3* to be expressed in corneal stromal keratocytes, again using RNA-seq data.[18] Functional studies will elucidate how the c.568G>C variant impacts the expression, localization, and function of PRDX3 in the cornea and whether or not the polychromatic crystalline-like opacities located in the stromal extra-cellular matrix are byproducts of aberrant PRDX3 proteins. To date, histopathologic examination of only one corneal button obtained post-mortem from an affected individual has been performed, which indicated that the opacities may represent focal lipid accumulations.[28]

According to the second edition of the IC3D classification of corneal dystrophies, PPPCD is currently classified as a subtype of PDCD as a category 4 dystrophy, indicating that "…the evidence for it, being a distinct entity is not yet convincing".[8] While the presence of punctate opacities anterior to Descemet membrane is a common feature of each subtype of PDCD, the PDCD subtypes differ in terms of inheritance, age of onset and morphology of the deposits. Herein, we present a comprehensive clinical characterization of PPPCD and report the association of a segregating *PRDX3* missense variant in four PPPCD pedigrees with an autosomal dominant inheritance pattern. Therefore, we suggest that PPPCD might be considered a distinct inherited disorder and reclassified as a category 1 dystrophy, defined as a "…well-defined corneal dystrophy in which the gene has been mapped and identified and the specific mutations are known." [8]

Supplementary Material

Refer to Web version on PubMed Central for supplementary material.

ACKNOWLEDGMENTS

This publication has been carried out in the framework of the Red Temática de Investigación Cooperativa en Salud (RETICS), reference number RD16/0008/0012, financed by the Instituto Carlos III - General Subdirection of Networks and Cooperative Investigation Centers (R&D&I National Plan 2008–2011) and the European Regional Development Fund (Fondo Europeo de Desarrollo Regional FEDER). Support also provided by National Eye Institute Grants R01 EY022082 (A.J.A.), P30 EY000331 (core grant), the Walton Li Chair in Cornea and Uveitis (A.J.A.), the Stotter Revocable Trust and an unrestricted grant to Stein Eye Institute from Research to Prevent Blindness.

The authors thank Dr. Carmen Cardona (Vissum Corporación, Alicante, Spain) for her support on the clinical assessment of the families included in the study.

Biography

Jorge L. Alió del Barrio MD, PhD, FEBOS-CR specialised in Ophthalmology at the Ramón y Cajal University Hospital (Madrid, Spain) and he has completed Cornea Fellowships at Guy's and St Thomas' Hospital and Moorfields Eye Hospital (London, UK). He is currently working as a surgeon in the Cornea, Cataract and Refractive Surgery Service of Vissum Corporación (Alicante, Spain). He is also Associate Professor at Universidad Miguel Hernández (Alicante, Spain) School of Medicine.

REFERENCES

1. Fernandez-Sasso D, Acosta JE, Malbran E. Punctiform and polychromatic pre-Descemet's dominant corneal dystrophy. Br J Ophthalmol 1979;63(5):336–338. [PubMed: 313810]
2. Lagrou L, Midgley J, Romanchuk KG. Punctiform and Polychromatophilic Dominant Pre-Descemet Corneal Dystrophy. Cornea 2016;35(4):572–575. [PubMed: 26845315]
3. Dolz-Marco R, Gallego-Pinazo R, Pinazo-Duran MD, Diaz-Llopis M. Crystalline subtype of pre-descemetic corneal dystrophy. J Ophthalmic Vis Res 2014;9(2):269–271. [PubMed: 25279130]
4. Coelho LM, Muinhos GK, Tanure MAG, Almeida HGd, Sieiro RdO. Distrofia policromática posterior da córnea. Revista Brasileira de Oftalmología 2015;74:186–188.
5. Tzelikis PFdM Santos URd, Tanure MAG Trindade FC. Distrofia corneana policromática posterior. Revista Brasileira de Oftalmologia 2007;66(4):262–266.
6. Lisch W, Weidle EG. [Posterior crystalline corneal dystrophy]. Klin Monbl Augenheilkd 1984;185(2): 128–131. [PubMed: 6332941]
7. Henríquez-Recine MA, Marquina-Lima KS, Vallespín-García E, García-Miñaur S, Benitez Del Castillo JM, Boto de Los Bueis A. Heredity and in vivo confocal microscopy of punctiform and polychromatic pre-Descemet dystrophy. Graefes Arch Clin Exp Ophthalmol 2018;256(9): 1661–1667. [PubMed: 29728753]
8. Weiss JS, Moller HU, Aldave AJ, et al. IC3D classification of corneal dystrophies-edition 2. Cornea 2015;34(2):117–159. [PubMed: 25564336]
9. Ng PC, Henikoff S. SIFT: Predicting amino acid changes that affect protein function. Nucleic Acids Res 2003;31(13):3812–3814. [PubMed: 12824425]
10. Adzhubei I, Jordan DM, Sunyaev SR. Predicting functional effect of human missense mutations using PolyPhen-2. Curr Protoc Hum Genet 2013;Chapter 7:Unit7 20.
11. Kircher M, Witten DM, Jain P, O'Roak BJ, Cooper GM, Shendure J. A general framework for estimating the relative pathogenicity of human genetic variants. Nat Genet 2014;46(3):310–315. [PubMed: 24487276]

12. Rentzsch P, Witten D, Cooper GM, Shendure J, Kircher M. CADD: predicting the deleteriousness of variants throughout the human genome. Nucleic Acids Res 2019;47(D1):D886–D894. [PubMed: 30371827]
13. Choi Y, Sims GE, Murphy S, Miller JR, Chan AP. Predicting the functional effect of amino acid substitutions and indels. PLoS One 2012;7(10):e46688. [PubMed: 23056405]
14. Desmet FO, Hamroun D, Lalande M, Collod-Beroud G, Claustres M, Beroud C. Human Splicing Finder: an online bioinformatics tool to predict splicing signals. Nucleic Acids Res 2009;37(9):e67. [PubMed: 19339519]
15. Baralle M, Baralle D, De Conti L, et al. Identification of a mutation that perturbs NF1 agene splicing using genomic DNA samples and a minigene assay. J Med Genet 2003;40(3):220–222. [PubMed: 12624144]
16. Pagani F, Stuani C, Tzetis M, et al. New type of disease causing mutations: the example of the composite exonic regulatory elements of splicing in CFTR exon 12. Hum Mol Genet 2003;12(10):1111–1120. [PubMed: 12719375]
17. Muro AF, Caputi M, Pariyarath R, Pagani F, Buratti E, Baralle FE. Regulation of fibronectin EDA exon alternative splicing: possible role of RNA secondary structure for enhancer display. Mol Cell Biol 1999;19(4):2657–2671. [PubMed: 10082532]
18. Frausto RF, Le DJ, Aldave AJ. Transcriptomic Analysis of Cultured Corneal Endothelial Cells as a Validation for Their Use in Cell-Replacement Therapy. Cell transplantation 2016;25(6):1159–1176. [PubMed: 26337789]
19. Li L, Shoji W, Takano H, et al. Increased susceptibility of MER5 (peroxiredoxin III) knockout mice to LPS-induced oxidative stress. Biochem Biophys Res Commun 2007;355(3):715–721. [PubMed: 17316558]
20. Shibata E, Nanri H, Ejima K, et al. Enhancement of mitochondrial oxidative stress and up-regulation of antioxidant protein peroxiredoxin III/SP-22 in the mitochondria of human pre-eclamptic placentae. Placenta 2003;24(6):698–705. [PubMed: 12828928]
21. Lee S, Wi SM, Min Y, Lee KY. Peroxiredoxin-3 Is Involved in Bactericidal Activity through the Regulation of Mitochondrial Reactive Oxygen Species. Immune Netw 2016; 16(6):373–380. [PubMed: 28035213]
22. Liu Z, Hu Y, Liang H, Sun Z, Feng S, Deng H. Silencing PRDX3 Inhibits Growth and Promotes Invasion and Extracellular Matrix Degradation in Hepatocellular Carcinoma Cells. J Proteome Res 2016;15(5):1506–1514. [PubMed: 26983019]
23. Hu JX, Gao Q, Li L. Peroxiredoxin 3 is a novel marker for cell proliferation in cervical cancer. Biomed Rep 2013;1(2):228–230. [PubMed: 24648924]
24. Kinnula VL, Lehtonen S, Sormunen R, et al. Overexpression of peroxiredoxins I, II, III, V, and VI in malignant mesothelioma. J Pathol 2002;196(3):316–323. [PubMed: 11857495]
25. Noh DY, Ahn SJ, Lee RA, Kim SW, Park IA, Chae HZ. Overexpression of peroxiredoxin in human breast cancer. Anticancer Res 2001;21(3B):2085–2090. [PubMed: 11497302]
26. Whitaker HC, Patel D, Howat WJ, et al. Peroxiredoxin-3 is overexpressed in prostate cancer and promotes cancer cell survival by protecting cells from oxidative stress. Br J Cancer 2013;109(4):983–993. [PubMed: 23880827]
27. Jurkunas UV, Rawe I, Bitar MS, et al. Decreased expression of peroxiredoxins in Fuchs' endothelial dystrophy. Invest Ophthalmol Vis Sci 2008;49(7):2956–2963. [PubMed: 18378575]
28. Croxatto J F-SD, Malbran ES. Clinicopathologic findings in punctiform and polychromatic pre-Descemet's corneal dystrophy. Invest Ophthalmol Vis Sci 2002;43(13):E-Abstract 1724.

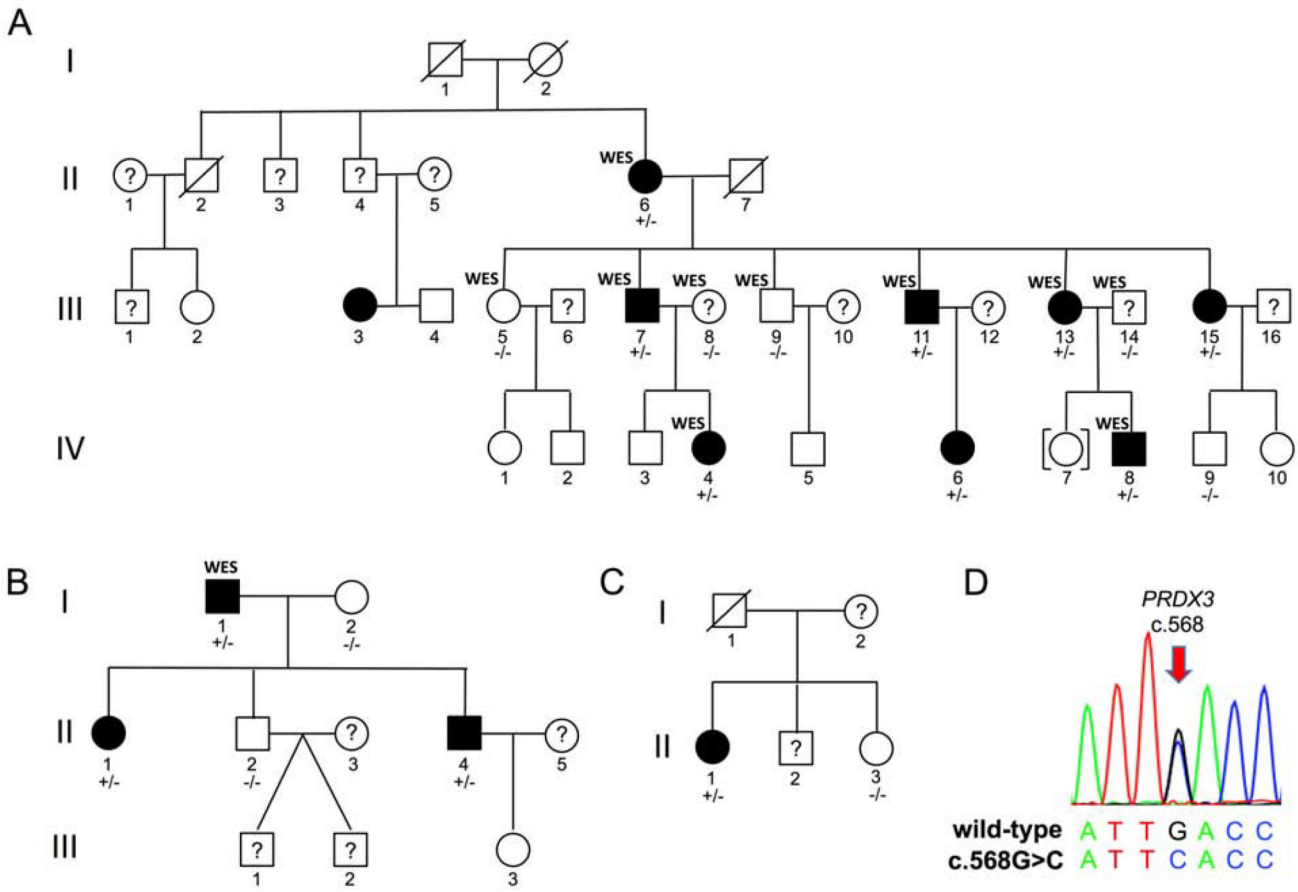

Figure 1.

Pedigrees of three previously unreported Spanish PPPCD families: family 1 (A), family 2 (B), and family 3 (C) with punctiform and polychromatic pre-Descemet corneal dystrophy. Question marks (?) indicate unexamined individuals. “WES” indicates individuals in whom whole exome sequencing was performed. Individuals heterozygous for the *PRDX3* c.568G>C variant are indicated by +/− and individuals who lack the variant are indicated by −/−. (D) The heterozygous *PRDX3* c.568G>C variant (Refseq: NM_006793.4) was confirmed by Sanger sequencing in all affected individuals.

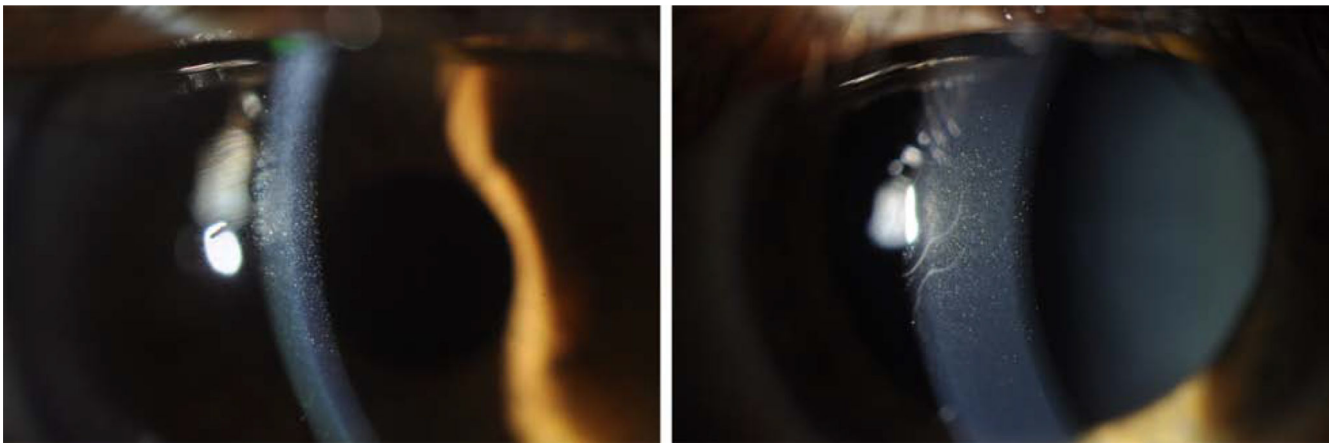

Figure 2.

Slit lamp photomicrographs of an individual with punctiform and polychromatic pre-Descemet corneal dystrophy (Figure 1A, III–15) demonstrating multiple polychromatic posterior stromal opacities in each eye.

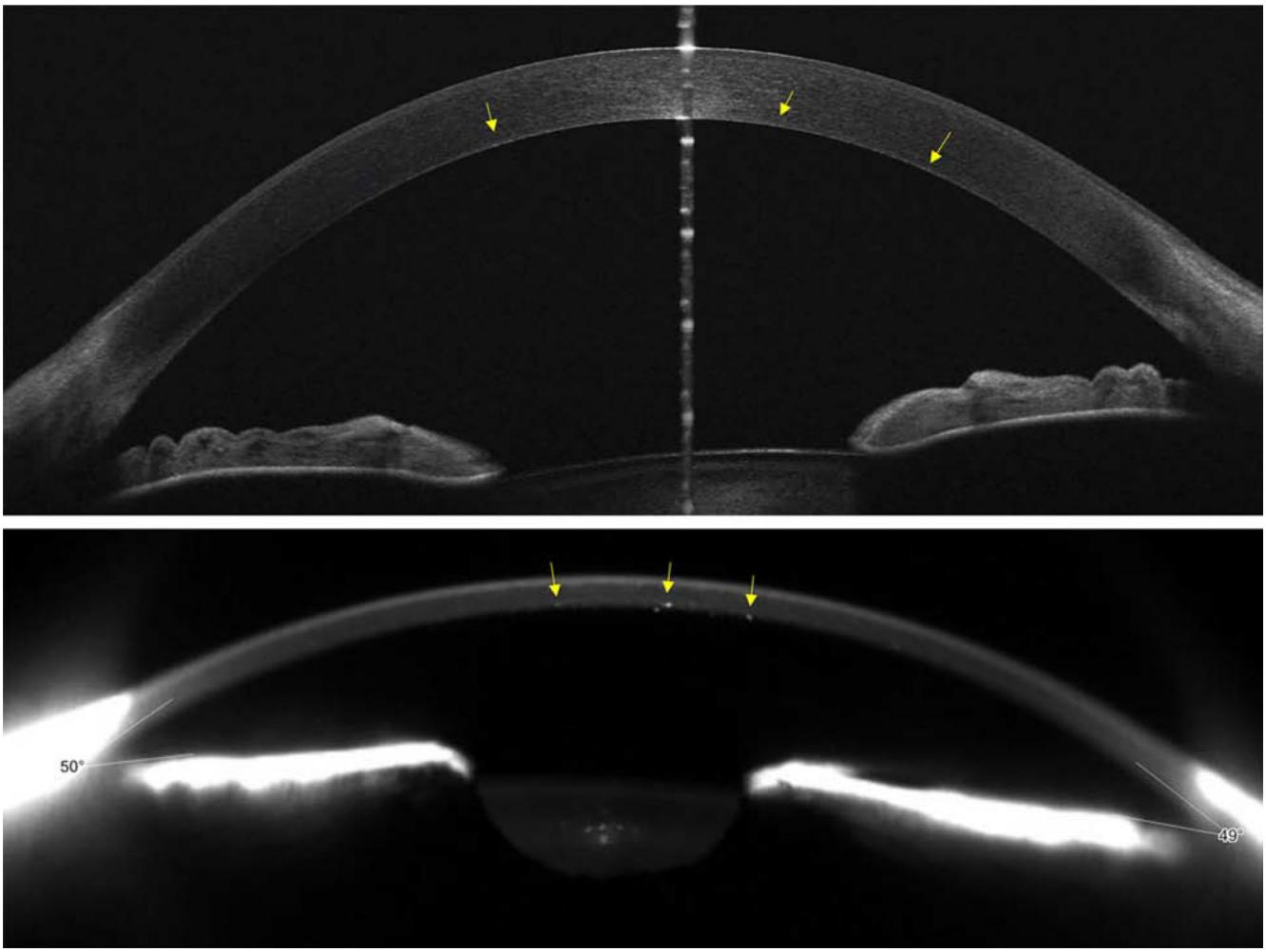

Figure 3.

Anterior segment OCT (top) and Scheimpflug (bottom) imaging of an individual with punctiform and polychromatic pre-Descemet corneal dystrophy (Figure 1A, III–11) demonstrating hyper-reflective posterior stromal opacities (indicated by yellow arrows) that are more easily identified with Scheimpflug imaging.

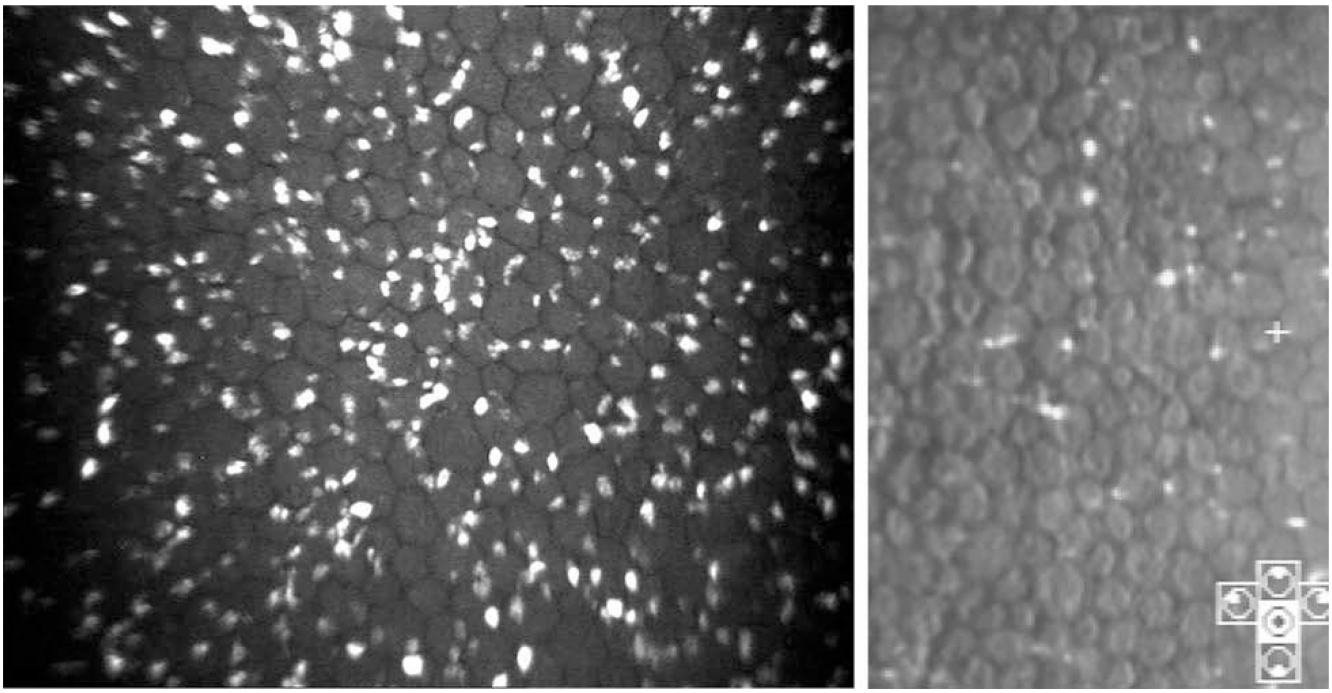

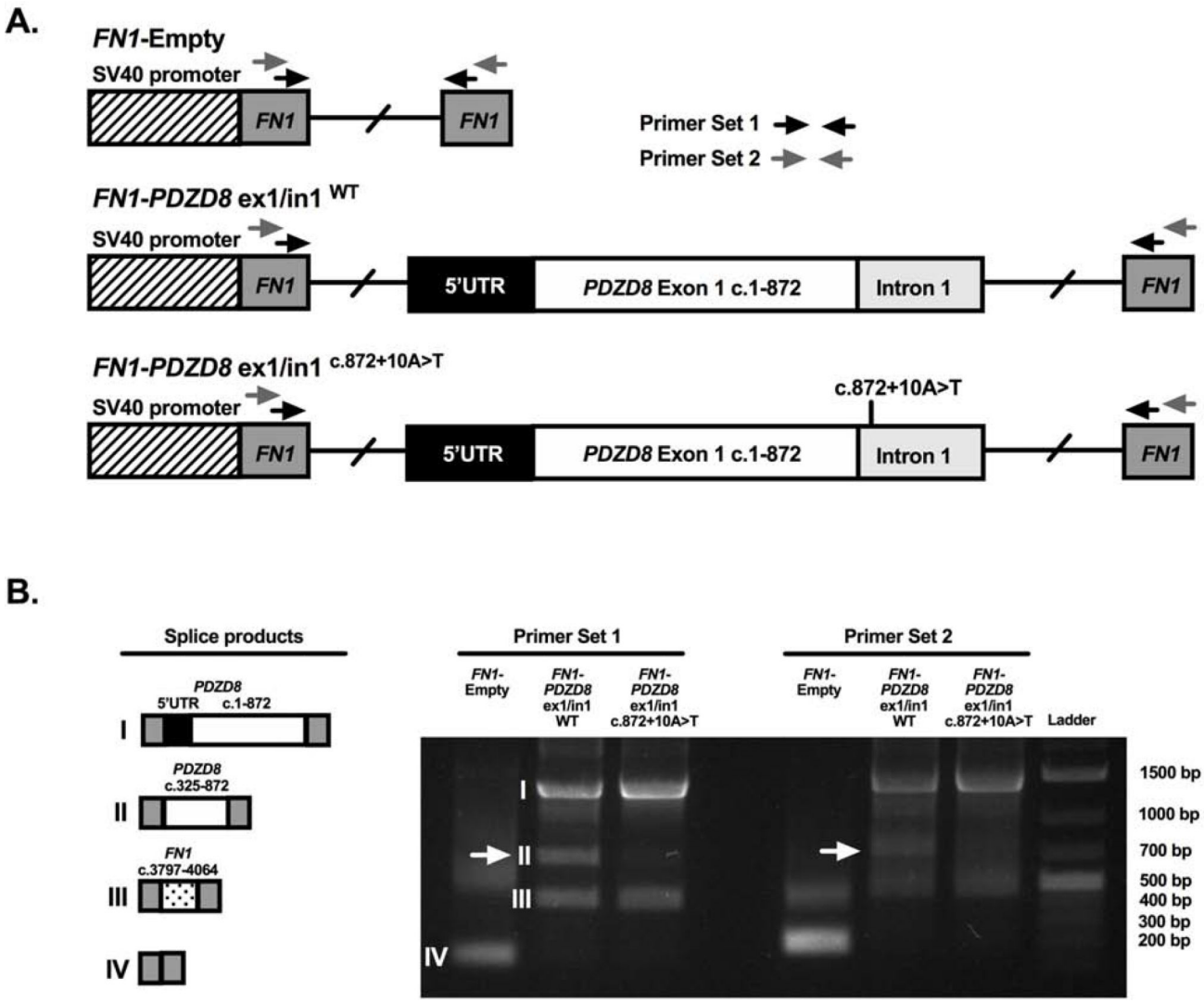

Figure 4.

Confocal microscopy (left) and specular microscopy (right) imaging of the posterior corneal stroma of an individual with punctiform and polychromatic pre-Descemet corneal dystrophy (Figure 1B, II–4) demonstrating hyper-reflective opacities distributed at the level of Descemet membrane.

Table 1.

Description of reported families with punctiform and polychromatic pre-Descemet corneal dystrophy in the literature.

Family	Authors	Country	Publication Year	Affected members	Proposed Inheritance	Family Origin
1	Fernandez-Sasso et al[1]	Argentina	1979	8	Autosomal dominant	French/Spanish Pyrenees
2	Lisch et al[6]	Germany	1984	2	Autosomal dominant	Non reported
3	Tzelikis et al[5]	Brazil	2007	3	Autosomal dominant	Non reported
4		Brazil	2007	1 (family members not analysed)	Non reported	Non reported
5	Dolz-Marco et al[3]	Spain	2013	2	Autosomal dominant	East Spain
6	Coelho et al[4]	Brazil	2015	1 (family members not analysed)	Non reported	Non reported
7		Brazil	2015	1 (family members not analysed)	Non reported	Non reported
8	Lagrou et al[2]	Canada	2016	3	Autosomal dominant	Columbia (USA) & Northern Spain (ancestral family)
9	Henriquez Recine et al[7]	Spain	2018	8	Autosomal dominant	Central Spain
10		Spain	2018	3	Autosomal dominant	Central Spain
11	Alió del Barrio et al	Spain	2019	9	Autosomal dominant	East Spain
12		Spain	2019	3	Autosomal dominant	East Spain
13		Spain	2019	1	Insufficient Sample	East Spain

Table 2.

Clinical evaluation of PPPCD families.

	PPPCD Affected		Unaffected		P Value
	Mean	**SD**	**Mean**	**SD**	
Refractive					
Ref Sphere (D)	−0.42	2.54	−2.08	3.26	0.12
Ref Cylinder (D)	−0.79	0.66	−0.48	0.45	0.1
CDVA (decimal)	0.1	0.05	1.02	0.06	0.43
Tomographic					
Anterior Km (D)	44.33	1.93	43. 94	1.35	0.67
Topo Cylinder (D)	−0.98	0.5	−1.13	0.44	0.2
CCT (μm)	528.65	30.69	539.4	25.48	0.24
Thinnest (μm)	517.75	32.81	530.15	28.27	0.21
Kmax (D)	44.83	1.96	44.51	1.43	0.74
Wavefont					
Corneal Total HOA (μm)	0.59	0.37	0.46	0. 1	0.35
Corneal Coma (μm)	0.33	0.18	0.31	0.1	0.95
Corneal Sph (μm)	0.22	0.18	0.22	0.07	0.11
Endothelial specular microscopy					
CD (cells/mm^2)	2563	708.7	2572	344.83	0.84
CV	43	40.3	33	5.56	0.12
Hexagonality (%)	61	10.13	61	9.26	0.48
Ocular abberometry					
Strehl Ratio (PSF)	0.37	0.15	0.39	0.17	0.85
OSI	1.24	1.19	0.82	0.53	0.62
Biomechanical					
CH (mm Hg)	10.32	1.44	9.85	1.52	0.26
CRF (mm Hg)	10.77	1.32	9.93	1.24	0.02 *
Intraocular Pressure					
IOP (mm Hg)	14.6	3.5	13.25	2.15	0,22

Ref: refractive; D: diopters; CDVA: corrected distance visual acuity; dec: decimal scale; Km: mean keratometry; Topo: topographic; CCT: central corneal thickness; Thinnest: thinnest pachymetric point; Kmax: maximum keratometry; HOA: higher order aberrations; Sph: spherical aberration; CD: cell density; CV: coefficient of variation; 6A: hexagonality; PSF: point spread function; OSI: ocular scatter index; CH: corneal hysteresis; CRF: corneal resistance factor].

* statistically significant differences.

Table 3.

Variants identified by WES

# of affecteds containing variant by WES	# of unaffecteds containing variant by WES	Chr	Position	Gene	Transcript ID	Transcript Variant	Amino acid change	dbSNP ID	gnomAD MAF (%)	SIFT/ PolyPhen-2 Function Prediction	Confirmed by Sanger sequencing to be present in 6 of 6 affected and 0 of 4 unaffecteds?	If confirmed by Sanger sequencing, does variant segregate in 3 additional family members?
6 of 6	0 of 4	10	117374346	*PDZD8*	NM_173791.4	c.872+10A>T	-	rs201808439	0.006	-	Yes	Yes
6 of 6	0 of 4	18	21505785	*GREB1L*	NM_001142966.2	c.4229-25T>C	-	rs775835476	0.004	-	Yes	No
5 of 6	0 of 4	1	248145920	*OR2M5*	NM_001004690.1	c.773T>C	p.M258T	rs146014040	0.056	Activating/ Benign	Yes	Yes
5 of 6	0 of 4	5	194925	LRRC14B	NM_001080478.2	c.1117 G>A	p.V373I	rs200063605	0.077	Tolerated/ Benign	No	-
5 of 6	0 of 4	5	10280458	CMBL	NM_138809.3	c.733A>C	p.M245L	rs182773279	0.086	Tolerated/ Benign	No	-
5 of 6	0 of 4	7	150692529	*GIMAP2*	NM_015660.2	c.243G>A	p.M81I	rs927523889	-	Activating/ Benign	No	-
5 of 6	0 of 4	8	8702651	CLDN23	NM_194284.2	c.253G>A	p.V85I	rs372410779	0.005	Tolerated/ Benign	No	-
5 of 6	0 of 4	10	17796225	TMEM236	NM_001098844.2	c.777C>A	p.N259K	rs1001234857	0.037	Tolerated/ Benign	No	-
5 of 6	0 of 4	10	119169326	*PRDX3*	NM_006793.4	c.568G>C	p.D190H	None	-	Damaging/ Prob. Dama.	Yes	Yes
5 of 6	0 of 4	18	23784125	*LAMA3*	NM_001127717.2	c.1571 G>A	p.R524H	rs201845068	0.036	None/Poss. Damaging	Yes	No
6 of 6	1 of 4	1	226736078	*ITPKB*	NM_002221.3	c.1381C>T	p.P461S	rs35823273	0.396	Tolerated/ Benign	No	-
6 of 6	1 of 4	7	74120997	*LIMK1*	NM_002314.3	c.1729C>T	p.P577S	rs147218553	0.018	Tolerated/ Benign	No	-
6 of 6	1 of 4	7	76482982	*DTX2*	NM_001102596.1	c.743A>G	p.N248S	rs145151450	0.314	Tolerated/ Benign	No	-